

PHYSICAL REVIEW B

CONDENSED MATTER AND MATERIALS PHYSICS

THIRD SERIES, VOLUME 58, NUMBER 12

15 SEPTEMBER 1998-II

RAPID COMMUNICATIONS

Rapid Communications are intended for the accelerated publication of important new results and are therefore given priority treatment both in the editorial office and in production. A Rapid Communication in Physical Review B may be no longer than four printed pages and must be accompanied by an abstract. Page proofs are sent to authors.

Nonlocal dynamical correlations of strongly interacting electron systems

M. H. Hettler, A. N. Tahvildar-Zadeh, and M. Jarrell

Department of Physics, University of Cincinnati, Cincinnati, Ohio 45221

T. Pruschke

Institut für Theoretische Physik, Universität Regensburg, Regensburg, Germany

H. R. Krishnamurthy

Department of Physics, Indian Institute of Science, Bangalore 560012, India

(Received 3 June 1998)

We introduce an extension of the dynamical mean-field approximation (DMFA) that retains the causal properties and generality of the DMFA, but allows for systematic inclusion of nonlocal corrections. Our technique maps the problem to a self-consistently embedded cluster. The DMFA (exact result) is recovered as the cluster size goes to 1 (infinity). As a demonstration, we study the Falicov-Kimball model using a variety of cluster sizes. We show that the sum rules are preserved, the spectra are positive definite, and the nonlocal correlations suppress the charge-density wave transition temperature. [S0163-1829(98)51436-1]

INTRODUCTION

Strongly interacting electron systems have been on the forefront of theoretical and experimental interest for several decades. This interest has intensified with the discovery of a variety of heavy-fermion and related non-Fermi-liquid systems and the high- T_c superconductors. In all these systems strong electronic interactions play a dominant role in the selection of at least the low temperature phase. The simplest theoretical models of strongly correlated electrons, the Hubbard model (HM) and the periodic Anderson model (PAM), have remained unsolved in more than one dimension despite a multitude of sophisticated techniques introduced since the inception of the models.

With the ground-breaking work by Metzner and Vollhardt¹ it was realized that these models become significantly simpler in the limit of infinite dimensions $D=\infty$. Namely, provided that the kinetic energy is properly rescaled as $1/\sqrt{D}$, they retain only local, though nontrivial, dynamics: The self-energy is constant in momentum space, though it has a complicated frequency dependence. Consequently, the HM and PAM map onto a generalized single impurity

Anderson model. The thermodynamics and phase diagram have been obtained numerically by quantum Monte Carlo (QMC) and other methods.²⁻⁴

The name dynamical mean-field approximation (DMFA) has been coined for approximations in which a purely local self-energy (and vertex function) is assumed in the context of a finite-dimensional electron system. While it has been shown that this approximation captures many key features of strongly correlated systems even in a finite-dimensional context, the DMFA, which leads to an effective single site theory, has some obvious limitations. For example, the DMFA cannot describe phases with explicitly nonlocal order parameters, such as d -wave superconductivity, nor can it describe the short-ranged spin correlations seen in the metallic state. Consequently, there have been efforts to extend DMFA by inclusion of nonlocal correlations, which would correspond to $1/D$ corrections to the self-energy of the $D=\infty$ models.^{5,6} These attempts have been only partially successful because of the difficulties of formulating a causal⁷ theory out of nonlocal Green functions. The nonlocal Green functions do not have a negative-definite imaginary part, so any self-energy diagram constructed with them is not guaranteed to

preserve causality. In fact, in the work by Schiller and Ingersent⁶ on the Falicov-Kimball model (FKM) violations of the spectral sum rule occurred for moderately large values of the interaction strength.

In this work we introduce a new method that includes short-ranged dynamical correlations and allows for nonlocal order parameters. The method is an iterative self-consistency scheme on a finite-size cluster with periodic boundary conditions. The essential approximation is the assumption that the self-energy is only weakly momentum dependent so that it is well approximated on a coarse grid of cluster momentum points \mathbf{K} . This approximation will be very good in high dimensions, but in low dimensions its validity is less clear. However, in many correlated systems, the momentum dependence of the self-energy is believed to be less important than its energy dependence, since the physical properties are dominated by a weakly dispersive feature in the electronic spectra near the Fermi surface, as seen, e.g., in experiments on heavy-fermion systems.⁸

The paper is organized as follows. First, we briefly review the DMFA, which is reproduced by our method if we choose a cluster consisting of only a single site. We then describe the new technique that we name dynamical cluster approximation (DCA). Finally, we demonstrate the method by example of the Falicov-Kimball model.

DYNAMICAL MEAN-FIELD APPROXIMATION

The DMFA assumes that the self-energy is a purely local functional of the local Green's function only, $\Sigma_{i,j} = \Sigma_{i,i}(G_{i,i})\delta_{i,j}$. Consequently, the self-energy has no momentum dependence, and the lattice problem may be mapped onto a self-consistently embedded impurity problem. The resulting DMFA algorithm has the following steps.

(1) The procedure starts with a local host Green's function \mathcal{G} that includes self-energy processes at all lattice sites except at the "impurity" site \mathbf{i} under consideration. \mathcal{G} defines the undressed Green's function of a generalized Anderson impurity model that is then solved by some technique, e.g., the QMC method.

(2) Then $\Sigma_{i,i} = \mathcal{G}^{-1} - G_{imp}^{-1}$, where G_{imp} is the computed Green's function of the generalized Anderson impurity model.

(3) This self-energy is assumed to also be the self-energy of the lattice. Consequently, the local lattice Green's function follows from $G_{i,i} = (1/N)\Sigma_{\mathbf{k}}(G_o^{-1}(\mathbf{k}) - \Sigma_{i,i})^{-1}$, where $G_o(\mathbf{k})$ is the bare lattice Green function and N is the (infinite) number of points of the lattice.

(4) The iteration loop closes by defining the new $\mathcal{G}^{-1} = G_{i,i}^{-1} + \Sigma_{i,i}$. The iteration typically continues until $G_{i,i} = G_{imp}$ to within the desired accuracy, and the procedure may be shown to be completely causal.

DYNAMICAL CLUSTER APPROXIMATION

We consider a cluster of size $N_c = L^D$ with periodic boundary conditions. The corresponding first Brillouin zone is divided into N_c cells of size $(2\pi/L)^D$. The algorithm begins with a guess, usually zero, for the cluster self-energy $\Sigma_c(\mathbf{K})$ (here and in the following we suppress the frequency argument). We now define a Green function \bar{G} as

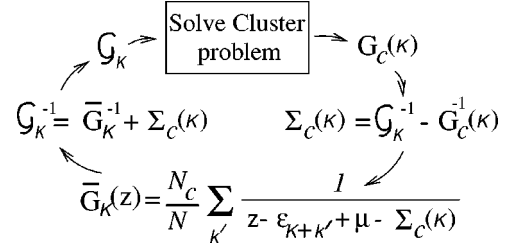


FIG. 1. Schematic sketch of the dynamical cluster algorithm.

$$\bar{G}(\mathbf{K}) = \frac{N_c}{N} \sum_{\mathbf{k}'} [z - \epsilon_{\mathbf{K}+\mathbf{k}'} + \mu - \Sigma_c(\mathbf{K})]^{-1}, \quad (1)$$

where the \mathbf{k}' summation runs over the momenta of the cell about the cluster momentum \mathbf{K} . z is the (complex) frequency argument, and μ the chemical potential. \bar{G} is causal provided that its proper self-energy $\Sigma_c(\mathbf{K})$ is causal. It is a coarse-grained average of the lattice Green's function in momentum space with a self-energy $\Sigma_c(\mathbf{K})$. Before a new estimate for the self energy can be formulated, we calculate the host cluster propagator $\mathcal{G}(\mathbf{K})$ using

$$\mathcal{G}^{-1}(\mathbf{K}) = \bar{G}^{-1}(\mathbf{K}) + \Sigma_c(\mathbf{K}). \quad (2)$$

This is the "cluster exclusion" to prevent overcounting of self-energy diagrams on the cluster. Since the self-energy in Eq. (1) is independent of the integration variable, Eqs. (1) and (2) are formally identical to the corresponding equations (steps 3 and 4) used in the DMFA (after rescaling \mathbf{k}'). Thus, at this point the DCA is equivalent to N_c independent DMFA's, one for each \mathbf{K} . That Eq. (2) preserves causality can be seen as follows: Since $\Sigma_c(\mathbf{K})$ in Eq. (1) does not depend on \mathbf{k}' , the sum on \mathbf{k}' can be rewritten as an energy integral with a \mathbf{K} -dependent density of states (DOS) $\rho_{\mathbf{K}}(\epsilon)$. However, for any positive semidefinite, normalized function $\rho_{\mathbf{K}}(\epsilon)$ one has

$$\int d\epsilon \frac{\rho_{\mathbf{K}}(\epsilon)}{z + \mu - \Sigma_c(\mathbf{K}) - \epsilon} = [z - \Sigma_c(\mathbf{K}) - \epsilon_{\mathbf{K}} + \mu - \Gamma_{\mathbf{K}}(z + \mu - \Sigma_c(\mathbf{K}))]^{-1}$$

with an effective "dispersion" $\epsilon_{\mathbf{K}} = (N_c/N)\Sigma_{\mathbf{k}'}\epsilon_{\mathbf{K}+\mathbf{k}'}$ for the embedded cluster and a causal function $\Gamma_{\mathbf{K}}(z + \mu - \Sigma_c(\mathbf{K}))$,⁹ which is the self energy of \mathcal{G} .

Given a causal host cluster propagator $\mathcal{G}(\mathbf{K})$ we then compute the interacting cluster Green's function $G_c(\mathbf{K})$ (or self-energy Σ_c) by any convenient method. This introduces nonlocal interactions and correlations between the different momentum cells. $\Sigma_c(\mathbf{K})$ is obtained via

$$\Sigma_c(\mathbf{K}) = \mathcal{G}^{-1}(\mathbf{K}) - G_c^{-1}(\mathbf{K}). \quad (3)$$

$\Sigma_c(\mathbf{K})$ is assumed to be a good approximation of the lattice self-energy at the cluster momenta. It is fed into Eq. (1) to generate a new $\bar{G}(\mathbf{K})$. This process is repeated until upon convergence of the algorithm $\bar{G}(\mathbf{K}) = G_c(\mathbf{K})$. The schematics of the algorithm is sketched in Fig. 1.

DISCUSSION OF THE ALGORITHM

Several assumptions were made in the construction of this algorithm. The first is the weak momentum dependence of the self-energy that is equivalent to assuming that the dynamical intersite correlations have some short spatial range $b \lesssim L/2$. Then, according to Nyquist's sampling theorem,¹⁰ to reproduce these correlations in the self-energy, we need only sample the reciprocal space at an interval of $\Delta k \approx 2\pi/L$; i.e., on a cluster of $N_c = L^D$ points within the first Brillouin zone. Equivalently, $\Sigma(\mathbf{K} + \mathbf{k}') \approx \Sigma(\mathbf{K})$ for each \mathbf{k}' within a cell of size $(\pi/b)^D$, so the lattice self-energy is well approximated by the self-energy $\Sigma_c(\mathbf{K})$ obtained from the coarse-grained cluster. Thus, the algorithm is a natural extension of the DMFA. The second assumption is the form of Eq. (1). This choice is not unique, but it is the simplest that maintains causality and produces an algorithm that both recovers the DMFA when $N_c = 1$ and becomes exact when $N_c = \infty$. When $N_c = 1$, the \mathbf{k}' summation runs over the complete Brillouin zone and \bar{G} is the local Green's function. When $N_c = \infty$, the \mathbf{k}' summation vanishes.

We want to stress that the DCA is a general scheme not specialized to a particular model of interest or to the technique used to obtain the cluster self-energy. A variety of techniques, including perturbation theory¹¹ [noncrossing approximation (NCA), the fluctuation exchange approximation¹²], quantum Monte Carlo, or numerical renormalization group can also be used to solve the embedded cluster problem.

APPLICATION: THE FALICOV-KIMBALL MODEL

The spinless FKM can be considered as a simplified Hubbard model in which one spin species is prohibited to hop and has consequently only local dynamics. The Hamiltonian reads

$$H = -t \sum_{\langle i,j \rangle} d_i^\dagger d_j - \mu \sum_i (n_i^d + n_i^f) + U \sum_i n_i^d n_i^f, \quad (4)$$

with $n_i^d = d_i^\dagger d_i$, $n_i^f = f_i^\dagger f_i$, and in the particle-hole symmetric case that we consider, $\mu = U/2$. We measure energies in units of the hopping element t . For $D \geq 2$ the system has a phase transition from a homogeneous high-temperature phase with $\langle n_i^d \rangle = \langle n_i^f \rangle = 1/2$ to a checkerboard phase [a charge density wave with ordering vector $\mathbf{Q} = (\pi, \pi, \dots)$] with $\langle n_i^d \rangle \neq \langle n_i^f \rangle$ for $0 < U < \infty$.¹³ In contrast to the Hubbard and related models, within the DCA the FKM can be solved without the application of QMC because the f electrons are static, acting as an annealed disorder potential on the dynamic d electrons. We generalize the algorithm of Brandt and Mielsch¹⁴ to a finite-size cluster. Given an initial host Green's function \mathcal{G}_{ij} of the d electrons, the algorithm first computes the Boltzmann weights w_f of all configurations $\{f\}$ of f electrons on the cluster, as $w_f = w_f^0/Z$ with

$$w_f^0 = 2^{N_c} \prod_{\omega_n} \det \frac{\bar{\mathcal{G}}_{ij}^{-1}(i\omega_n) - U n_i^f \delta_{ij}}{i\omega_n \delta_{ij}} \quad (5)$$

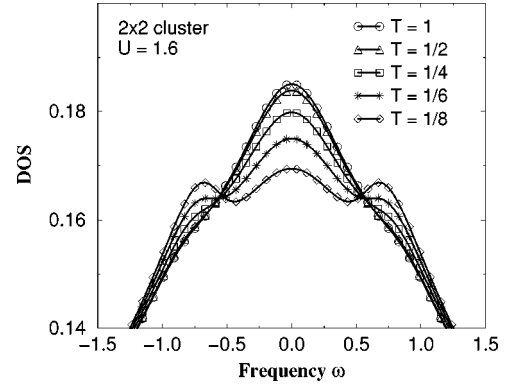


FIG. 2. Conduction electron DOS in the homogeneous phase for various temperatures (2×2 cluster) and $U = 1.6$. Note the emergence of “charge-transfer” peaks with simultaneous suppression of the 2D van Hove peak at the band center. In contrast, the DMFA result is temperature independent.

the unnormalized weight. $Z = \sum_{\{f\}} w_f^0$ is the “partition sum.” The determinant is to be taken over the spatial indices. Given the weights, the new d -electron cluster Green's function is given by

$$\mathcal{G}_{ij}(z) = \sum_{\{f\}} w_f [\mathcal{G}_{ij}^{-1}(z) - U n_i^f \delta_{ij}]^{-1}. \quad (6)$$

The self-consistency loop closes by use of Eqs. (1)–(3).

Because the number of f configurations grows exponentially with the cluster size we confine ourselves to 1×1 , 2×2 , and 4×4 clusters in two dimensions. We first simultaneously determine the weights and the Matsubara Green's function. Then we use knowledge of the weights to find the retarded Green's function. Convergence of the algorithm is fast for Matsubara frequencies, but relatively slow for real frequencies. Upon convergence we test the sum rules of the spectral function at the cluster momenta.

The spectral functions are always positive, and the sum rules for both the cluster Green's function as well as the host Green's function \mathcal{G} are fulfilled within numerical accuracy for moderate interaction strength U . For large U a gap opens in the DOS and convergence becomes more difficult for $\omega = 0$. This is because the self-energy for the momenta on the Fermi surface [e.g., $\mathbf{K} = (\pi, 0)$] approaches the atomic limit $\Sigma(\omega) \approx U^2/4(\omega + i\eta)$ for frequencies inside the gap (η is a positive infinitesimal). This implies that as $\omega \rightarrow 0$, $\text{Im} \Sigma \rightarrow -\infty$, which is rather difficult to converge to. On the other hand, for all other frequencies the algorithm converges to within the desired accuracy. Since the contribution to the DOS from $\omega = 0$ is infinitesimal, the spectral sum rules are also fulfilled to within numerical accuracy. We emphasize that these peculiarities at $\omega = 0$ are only observed for the real frequency algorithm. For the Matsubara frequency algorithm, the sum rules (which may be reexpressed in terms of imaginary-time propagators) were always satisfied and the algorithm was perfectly stable (at least at the temperatures considered).

In Fig. 2 we show the DOS of the conduction electrons for the half-filled case for the 2×2 cluster for $U = 1.6$. In DMFA there is *no* temperature dependence of the DOS, since the weights of the unoccupied and occupied f state are

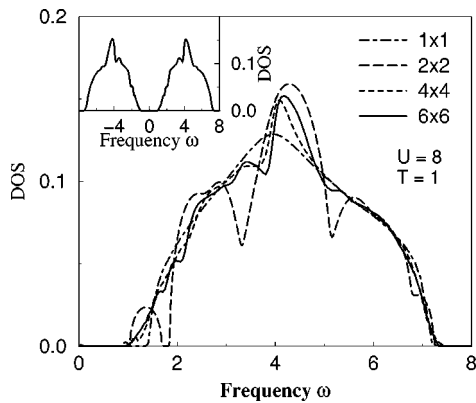


FIG. 3. Conduction electron DOS in the homogeneous phase for various cluster sizes for a fixed $T=1$ and $U=8$. Only half of the symmetric DOS is shown. Note that the artificial sideband of the 2×2 cluster disappears at larger cluster size. The entire DOS for the 6×6 cluster is shown in the inset.

$w_0 = w_1 = 1/2$, independent of temperature (in the homogeneous phase). This is changed in the DCA, where the checkerboard configurations begin to dominate as the temperature is lowered. The result is the appearance of the “charge transfer” features in the DOS, the two peaks separated by the interaction strength U .

Next, we explore the finite-size effects of the DCA at large U where the DOS shows more features (including a gap), and finite-size effects are more severe. In small clusters the effects of periodic boundary conditions are strong. Our results for the DOS at $U=8$ are shown in Fig. 3. Notice how the spurious features of the 2×2 cluster (strong dips and an additional small gap) have essentially disappeared in the DOS of the 4×4 cluster, though small features at the edges of the gap remain (not discernible in the figure). As larger clusters cannot be evaluated exactly (too many configurations) we employ Monte Carlo sampling of the configurations. As a preliminary result of work in progress we show the DOS of the 6×6 cluster. Already at this modest cluster size all finite-size features are essentially eliminated. This hints to the superior finite-size scaling properties of the DCA as compared to the standard lattice techniques without coupling to a host.

Finally, we discuss the effect of nonlocal corrections on the transition temperature T_c to the checkerboard phase. Within the DCA, we find T_c by estimating the temperature where the order parameter in the broken symmetry phase vanishes. The phase diagram is displayed in Fig. 4. The nonlocal correlations of the DCA suppress the T_c compared to the DMFA estimate, except for weak U where the nonlocal corrections to the vertex are very small (of order U^2 smaller than local contributions). For large U , however, the model

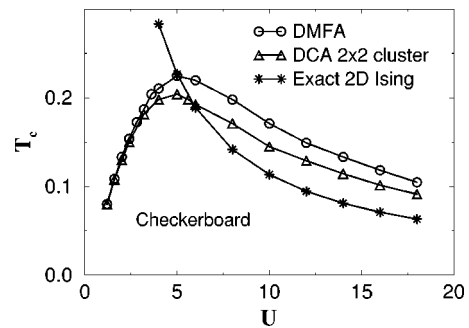


FIG. 4. Phase diagram of the 2D FKM at half filling. Compared to the DMFA result (circles) T_c of the 2×2 cluster DCA (triangles) is significantly suppressed for large interaction. At asymptotically large U the T_c of the DCA is bounded from below by the T_c of the 2D Ising model.

maps onto an effective Ising model with a near-neighbor exchange coupling $J = t^2/2U$ and a corresponding $T_c^{Ising} = 1.134/U$.¹⁵ Figure 4 shows that already for the 2×2 cluster the achieved correction takes one almost halfway to the asymptotically ($U \rightarrow \infty$) exact T_c of the two-dimensional (2D) Ising model.

CONCLUSIONS

We have introduced a new dynamical cluster approximation that includes short-ranged spatial correlations in addition to the local correlations of the dynamical mean-field approximation of strongly interacting electron systems. The method interpolates between the infinite lattice and the DMFA by evaluating the self-energy on a finite-size cluster with periodic boundary conditions. The DCA is a general scheme and is easily adapted to specific models and various existing exact and perturbative techniques to solve these models. As an example we applied the method to the Falicov-Kimball model in 2D and obtained the DOS as a function of temperature for small cluster sizes. In addition, we computed the critical temperature of the checkerboard phase transition and showed that it is suppressed for large interactions when compared to the result of DMFA.

ACKNOWLEDGMENTS

It is a pleasure to acknowledge discussions with J. Freericks, G. Baker, P. G. J. van Dongen, J. Gubernatis, A. Schiller and F.-C. Zhang. This work was supported by NSF Grant Nos. DMR-9704021 and DMR-9357199, and by the Ohio Board of Regents (H.R.K.). Travel support was provided by NATO (T.P. and M.J.). Computer support was provided by the Ohio Supercomputer Center.

¹W. Metzner and D. Vollhardt, Phys. Rev. Lett. **62**, 324 (1989).

²M. Jarrell, Phys. Rev. Lett. **69**, 168 (1992).

³T. Pruschke, M. Jarrell, and J. K. Freericks, Adv. Phys. **42**, 187 (1995).

⁴A. Georges, G. Kotliar, W. Krauth, and M. Rozenberg, Rev. Mod. Phys. **68**, 13 (1996).

⁵P. G. J. van Dongen, Phys. Rev. B **50**, 14 016 (1994).

⁶A. Schiller and K. Ingersent, Phys. Rev. Lett. **75**, 113 (1995).

⁷By causal we mean that the spectral function is positive semidefinite and that it preserves the sum rule.

⁸A. B. Andrews *et al.*, Phys. Rev. B **53**, 3317 (1996).

⁹This is a simple consequence of the fact that for any positive

semidefinite function the Hilbert transform can be represented as continued fraction with positive coefficients in the numerator of each of the fractions.

- ¹⁰D. F. Elliot and K. R. Rao, *Fast Transforms: Algorithms, Analyses, Applications* (Academic Press, New York, 1982).
- ¹¹N. S. Vidhyadhiraja, M. H. Hettler, M. Mukherjee, T. Pruschke, M. Jarrell, and H. R. Krishnamurthy (unpublished).

- ¹²N. E. Bickers and D. J. Scalapino, *Ann. Phys. (N.Y.)* **193**, 206 (1993).
- ¹³U. Brandt and R. Schmidt, *Z. Phys. B* **63**, 45 (1986); **67**, 43 (1987).
- ¹⁴U. Brandt and C. Mielsch, *Z. Phys. B* **75**, 365 (1989).
- ¹⁵P. G. J. van Dongen, *Phys. Rev. B* **45**, 2267 (1992).